

# Evaluation of Souss-Massa Daraa Region Irrigation Groundwater Hydrogeochemical Characteristics and Quality: A Multivariate Statistical Approach

M. Doubi<sup>1</sup>, H. Darif<sup>2</sup>, A. Koulou<sup>3</sup>, R. Tourir<sup>3,4\*</sup>,  
H. Abba<sup>5</sup>, M. Khaffou<sup>5</sup> and H. Erramli<sup>1</sup>

<sup>1</sup>Organic chemistry, catalysis and environment laboratory, Faculty of Sciences, Ibn Tofail University, Kenitra, Morocco

<sup>2</sup>Laboratory of Biotechnology, Environment and Quality (LABEQ), Faculty of Sciences, Ibn Tofail University, Kenitra, Morocco

<sup>3</sup>Advanced Materials and Process Engineering Laboratory, Faculty of Sciences, Ibn Tofail University, Kenitra, Morocco

<sup>4</sup>Regional Center for Education and Training Professions (CRMEF), Kenitra, Morocco.

<sup>5</sup>Higher School of Technology, Khénifra, Morocco

\*Corresponding author: tourir8@yahoo.fr, tourir8@gmail.com

Received 12/09/2021; accepted 25/11/2022

<https://doi.org/10.4152/pea.2022400603>

---

## Abstract

The quality of the Souss-Massa Daraa (S-MD) aquifer is influenced by natural and anthropogenic contaminations. Indeed, geological formations are the main sources of mineralization in the aquifer, which compromises the potential irrigation, and threatens the sustainability of agricultural activities. In this context, hydrochemical and statistical studies were carried out on the major and secondary elements of water, based on different physico-chemical parameters, such as T °C, pH, EC (electric conductivity), NO<sub>3</sub><sup>-</sup> (nitrate), Cl<sup>-</sup> (chloride), HCO<sub>3</sub><sup>-</sup> (bicarbonate), SO<sub>4</sub><sup>2-</sup> (sulfate), Ca<sup>2+</sup> (calcium ions), Mg<sup>2+</sup> (magnesium ions), K<sup>+</sup> (potassium ion), Na<sup>+</sup> (sodium), Na%, Mg% and SAR (sodium adsorption ratio). The sampling was carried out in 2018, over two seasons (winter and summer), by analyzing 26 wells distributed over the studied plain.

According to the water classification based on EC, it was found that 80% of the samples show very high mineralization, and 96.66% are very hard and unfit for human consumption. Also, Cl<sup>-</sup> values of most of the samples were within limits inappropriate for irrigation, but some estimated parameters, such as Na% and SAR, were within appropriate levels. In addition, according to the piper diagram, the waters are characterized by a geochemical facies of 86.66% NaCl (sodium chloride), 13.33% CaSO<sub>4</sub> (sulphated calcium) and Mg. Thus, the principal component analysis (PCA) shows that the region waters mineralization is of natural origin.

**Keywords:** Souss-Massa Daraa aquifer, hydrogeochemical and statistical studies, Piper and Wilcox's diagrams, water quality, facies, and agricultural activities.

---

## Introduction

Groundwater is the most expensive natural resource; it is the main source for drinking water, industrial activities, agriculture, etc. [1, 2]. Over the past decades,

the demand for irrigation water has increased worldwide. Globally, around 43% of groundwater is used for agricultural irrigation, and this will increase up to 14% by 2030 [3]. To meet the ever-increasing water needs of the demographic explosion, and agricultural and industrial extension of Moroccan cities, the excessive withdrawal of groundwater has resulted in the depletion and deterioration of underground aquifers [3-6].

In the S-MD area, intensive agricultural activities are considered among the potential sectors that may contribute to water and soil quality degradation. Domestic and industrial discharges are also major sources of surface water pollution, which can infiltrate and contaminate groundwater. Groundwater contamination can cause danger to human health. In addition, the use of uncontrolled water for irrigation is a significant environmental problem, due to its direct impact on plant growth and crop yields and, therefore, on human and animal health. For this reason, it is necessary to examine and control the groundwater quality, prevent and reduce pollution and provide means of protecting and determining treatment processes, since this is necessary to produce water acceptable for consumption. In fact, continuous monitoring and evaluation of the groundwater quality helps to save lives and the environment [7, 8].

Several statistical methods and models have been employed for the assessment of groundwater quality and quantity in the world. For example, multivariate statistical techniques help to identify the possible factors/sources that influence water systems, and offer a robust tool for reliable water resources management, as well as a quick solution to pollution problems in many parts of the world [9, 10].

The goal of this study is to develop a reliable multi-statistical method to assess the impacts of the global change of recent years on the quality of groundwater samples of the S-MD region, which will be useful for decision-makers to take proper initiatives for agricultural irrigation.

## ***Materials and methods***

### ***Study Area***

The S-M basin is located in south-western Morocco, and it is one of the country most important hydrological catchments, with an area of 27 000 km<sup>2</sup>. Elevations in this catchment range from 0 m (Atlantic Ocean) to 4168 m (Toubkal peak in the High Atlas Mountains) [11]. It is situated between the Atlantic Ocean, the High Atlas and the Anti-Atlas Mountains (Fig. 1).

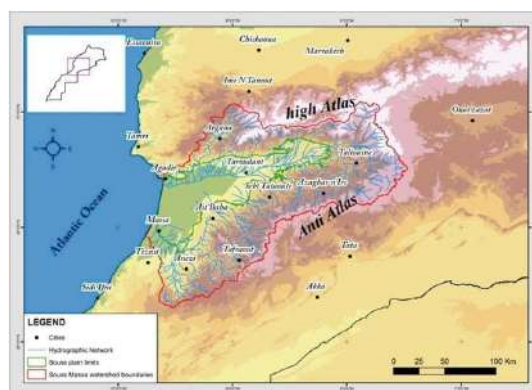


**Figure 1.** S-M basin geographical location.

In addition, the watershed of the studied area is composed of 25% of plains and 75% of mountains, and the main plain is Souss (4500 km<sup>2</sup>).

Three factors determine the semi-arid Mediterranean climate of the region, namely relief, ocean coast and the Sahara. Thus, the north of the region, dominated by Atlas, is characterized by a semi-arid to humid climate, progressing towards the plain. The plain, which occupies the Atlas sunken relief and the S-MD basin has an arid climate, despite a wide opening to the Atlantic. Finally, the southern and southeastern of the region that make up the south side are covered by the Sahara Desert climate. The precipitations are very varied in space and time, with a rainfall average of 200 mm/year [12]. On the other hand, the studied region is surrounded by two rivers, Souss from the north, and Massa from the south, giving to the area the name Souss-Massa. So, the Souss river takes in an important inflow generated from the High Atlas mountains, while Massa river receives an influx from the Anti-Atlas mountains [11].

### Geology description

The studied region is part of the S-M basin, which is located in the southern furrow of the Atlas belonging to the domain of the plains separating the High Atlas and the Anti-Atlas mountains. It was formed during the orogenic phases of Neogene and Quaternary. It is occupied by Cenozoic deposits represented by limestone and sub-horizontal clastic expanses of the Plio-Quaternaire, which form the SM-basin. Structurally, the Souss plain is a narrow rift zone with steep walls between the High Atlas and the Anti-Atlas. Formations of Plio-Quaternary calcareous clastic and marl fillings cover the East-West oriented Cretaceous-Eocene syncline.

The northern flank of this syncline outcrops in a discontinuous manner along the High Atlas. Its southern flank is characterized by a line of hills formed by Turonian limestone in the Souss plain axis. At the Issen river, the dominant Permo-Triassic classic is represented by conglomerates, sandstones, sandstone clays and red marl (1000 m thick). This basal succession is surmounted by gypsiferous and saline clays (500 m thick) (Figs. 2 and 3) [13].

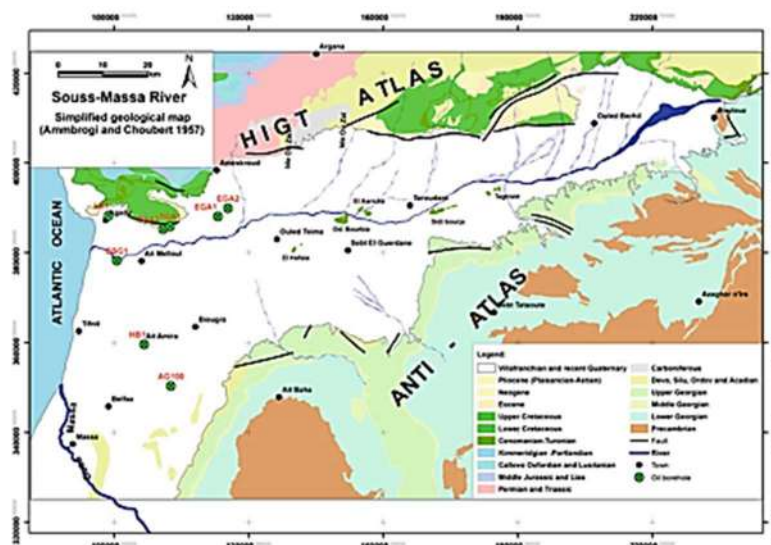


**Figure 2.** Geological schematic cross sections according to the S-M basin geophysics and drilling [13].

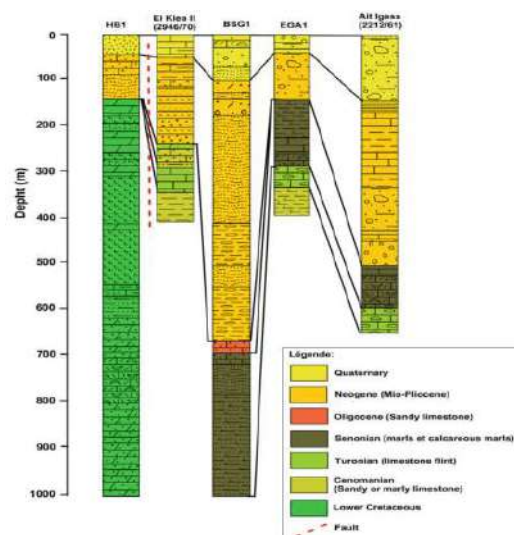


**Figure 3.** Logs of deep oil and hydrogeologic boreholes showing the S-M basin subsurface stratigraphy [13].

### ***Water sample collection and assessment***

Groundwater samples were collected twice a year (winter and summer seasons), from 26 preselected wells (shallow and deep), in 2018. All the samples were kept in polyethylene bottles and stored at 4 °C. Physico-chemical parameters, such as T (°C), pH and EC were measured *in situ*. Na, K (potassium), Ca and Mg elemental concentrations were analyzed by using an atomic absorption spectrophotometer (iCE-3000 AAS, Thermo scientific). In addition, HCO<sub>3</sub><sup>-</sup> and Cl<sup>-</sup> were analyzed by acid and silver nitrate (AgNO<sub>3</sub>) titration methods, respectively. Thus, the SO<sub>4</sub><sup>2-</sup> (sulfate ions) concentration was determined by the BaCl<sub>2</sub> (barium chloride) turbidity method, using a UV/Visible spectrophotometer (CE-7500, Cecil). The analytical procedures were followed as suggested by the American Public Health Association (APHA). The principal component analysis was performed using XLSTAT (statistical software for Excel, version 2017.1), to illustrate and summarize the variability in the data set, in terms of variables inter-correlation. Moreover, Piper and Wilcox's diagrams were prepared through Aqua-Chem (version 2011.1), to interpret hydrogeochemical facies (expressed as the measured concentration of major ions in decreasing order), and to classify the irrigation groundwater suitability, respectively.

To assess the use of irrigation water, various parameters, such as Na%, Mg%, SAR and RSC (residual sodium carbonate - Na<sub>2</sub>CO<sub>3</sub>), were determined.

## **Results and discussion**

### ***Physico-chemical parameters***

Fig. 4 represents the groundwater pH variation of the studied area, during two seasons (winter and summer). It is noted that pH varied from 8.22 to 6.95, and from 8.19 to 6.9, during the rainy and dry seasons, respectively, which indicates the pH alkaline nature in both of them, in the studied area. It is known that pH determines the physicochemical equilibrium between water, dissolved carbon dioxide (CO<sub>2</sub>), carbonates (CO<sub>3</sub><sup>2-</sup>) and HCO<sub>3</sub><sup>-</sup>, in the most natural waters [14]. On

the other hand, this parameter depends on the water origin, as well as on the geological nature of the type of land that water has crossed [14].

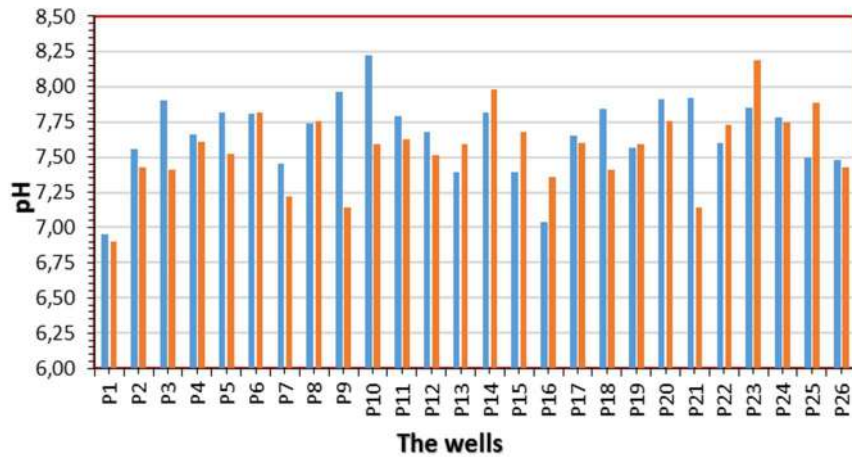


**Figure 4.** pH wells spatio-temporal variation in winter (January 2018) and summer (July 2018).

Fig. 5 represents the EC spatio-temporal variation during the two periods (rainy and drought). It is observed that the EC in the studied area ranged from 6390  $\mu\text{s}/\text{cm}$  to 547  $\mu\text{s}/\text{cm}$ , and from 6400  $\mu\text{s}/\text{cm}$  to 542  $\mu\text{s}/\text{cm}$ , during the rainy and dry seasons, respectively. It is also noted that five sites do not comply with the water quality standards in Morocco, indicating that they have very poor quality water, as their EC varies from 6400  $\mu\text{s}/\text{cm}$  to 3000  $\mu\text{s}/\text{cm}$ . The other sites have good to medium quality waters, since their EC is lower than 2700  $\mu\text{s}/\text{cm}$ .

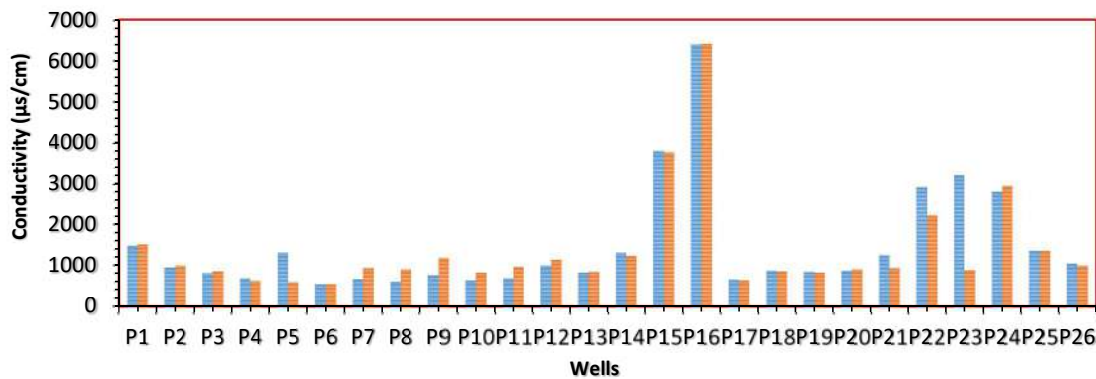


**Figure 5.** EC wells spatio-temporal variation during winter (January 2018) and summer (July 2018).

For example, at winter season (Table 1), it is observed that the cation concentrations of  $\text{Na}^+$ ,  $\text{K}^+$ ,  $\text{Ca}^{2+}$  and  $\text{Mg}^{2+}$  ions ranged from 30 mg/L (P4) to 690 mg/L (P16), 23 mg/L (P14) to 153 mg/L (P15), 48 mg/L (P17) to 348.6 mg/L (P16) and 1.3 mg/L (P25) to 7.9 mg/L (P16), respectively. So, the concentration of dissolved anions, such as  $\text{Cl}^-$ ,  $\text{HCO}_3^-$ ,  $\text{SO}_4^{2-}$ ,  $\text{NO}_3^-$  and  $\text{NO}_2^-$  (nitrogen dioxide), varied from 0.002 mg/L (P3) to 0.076 mg/L (P17), 215.94 mg/L (P5) to 826.54 mg/L (P1; P26), 25.7 mg/L (P6) to 722 mg/L (P22) and 3.28 mg/L (P17) to 81 mg/L (P24), respectively.

Moreover, according to some authors, the highest HCO<sub>3</sub><sup>-</sup> and Ca<sup>2+</sup> ion concentrations revealed that the study area might be influenced by HCO<sub>3</sub><sup>-</sup> mineral dissolution [8]. In addition, Holland pointed out that 74 ± 10% Ca<sup>2+</sup> and 40 ± 20% Mg<sup>2+</sup> in the groundwater derived from HCO<sub>3</sub><sup>-</sup> minerals dissolution, rather than from silicate (SiO<sub>2</sub> or SiO<sub>4</sub>) minerals [15].

The general characteristics of the S-M region groundwater physicochemical parameters, during winter and summer, are shown in Tables 1 and 2.

**Table 1.** Different S-M groundwater physicochemical parameters, during high water periods (January 2018: winter).

Wells	pH	T <sub>eau</sub> °C	T <sub>air</sub> °C	CE (µs/cm)	O <sub>2</sub> (mg/L)	SO <sub>4</sub> <sup>2-</sup> (mg/L)	Cl <sup>-</sup> (mg/L)	NO <sub>3</sub> <sup>-</sup> (mg/L)	NO <sub>2</sub> <sup>-</sup> (mg/L)	HCO <sub>3</sub> <sup>-</sup> (mg/L)	Na <sup>+</sup> (mg/L)	K <sup>+</sup> (mg/L)	Ca <sup>2+</sup> (mg/L)	Mg <sup>2+</sup> (mg/L)
P1	6.95	22.40	21.50	1482	5.93	110.6	88.75	23.5	0.019	862.54	54	7.5	156	81.5
P2	7.56	24.60	28.00	945	7.69	146.6	35.5	10.8	0.015	375.5	43	2.3	140	27.5
P3	7.90	24.80	28.20	803	7.9	102.4	44.37	11.4	0.002	363.54	42	3.7	92.18	46.6
P4	7.66	21.70	29.00	675	7.71	72.21	42.6	8.17	0.018	351.36	30	3.2	105	34
P5	7.82	23.90	27.90	1310	8.66	75.93	179.27	3.8	0.024	215.94	51	2.7	78.74	38
P6	7.81	22.40	28.50	547	8.16	25.7	53.25	11.57	0.036	278.16	30	1.7	67.43	17.7
P7	7.45	22.50	22.80	658	7.75	108	28.4	14.79	0.020	307.44	33	2.9	64	46.6
P8	7.74	23.30	27.00	606	8	56.6	21.3	8.8	0.041	283.04	32	2.5	68	27.9
P9	7.96	24.10	24.90	761	7.96	49.16	87	19.24	0.015	340.4	32	3.6	88	55
P10	8.22	24.20	27.60	639	9.34	70.3	35.5	10.6	0.032	296.46	37	3.3	72	32
P11	7.79	24.60	28.60	679	7.99	109	35.5	5.8	0.025	267.66	35	1.9	90	31
P12	7.68	21.00	19.50	996	7.89	69.5	122.4	8.89	0.016	360.9	52	3.2	100	58
P13	7.39	25.70	32.00	816	6.18	64.6	138.5	9.76	0.017	370	54	2.5	92	48
P14	7.82	21.10	26.00	1310	6.4	107.5	243.2	7.15	0.008	270	175	5.2	112	23
P15	7.39	25.10	26.20	3780	7.61	306.6	825.5	11.48	0.026	407.48	400	7.2	206	153
P16	7.04	25.20	26.80	6390	2.03	570	1597.5	19.7	0.012	318.45	690	7.9	348.6	133
P17	7.65	27.10	23.50	651	6.85	36.5	49.7	3.28	0.076	283.04	68	2.5	48	25.6
P18	7.84	26.20	30.20	875	7.55	140	92.3	14.40	0.005	402.6	41	3.2	76	48.4
P19	7.57	25.80	21.50	842	7.57	38.682	60.35	26.90	0.038	379.42	36	2.7	78	45.4
P20	7.91	25.90	30.90	876	7.54	64	124.2	26.6	0.009	314	70	2.8	75	55
P21	7.92	24.30	24.20	1250	8.29	58.5	181	10.26	0.064	256.2	116	2.2	75	36
P22	7.60	25.20	25.00	2910	6.2	722	399	15	0.012	270.8	335	3.8	246	80.6
P23	7.85	19.00	26.00	3200	6.5	460	316	47.8	0.053	390	142.5	4.1	153	113
P24	7.78	22.40	21.20	2790	8	38	582.2	81	0.014	350.14	210	2.4	145	112
P25	7.50	24.00	23.00	1355	6.44	35.8	223.65	21	0.024	356.24	126	1.3	96.19	50.8
P26	7.48	23.90	21.50	1482	5.93	110.6	88.75	23.5	0.019	862.54	54	7.5	156	81.5

**Table 2.** Different S-M groundwater physicochemical parameters, during low water periods (July 2018: summer).

Wells	Ph	T <sub>water</sub> °C	T <sub>air</sub> °C	CE (µs/cm)	O <sub>2</sub> (mg/L)	SO <sub>4</sub> <sup>2-</sup> (mg/L)	Cl <sup>-</sup> (mg/L)	NO <sub>3</sub> <sup>-</sup> (mg/L)	NO <sub>2</sub> <sup>-</sup> (mg/L)	HCO <sub>3</sub> <sup>-</sup> (mg/L)	Na <sup>+</sup> (mg/L)	K <sup>+</sup> (mg/L)	Ca <sup>2+</sup> (mg/L)	Mg <sup>2+</sup> (mg/L)
P1	6.90	23.30	39.30	1519	5.46	191	63.9	13.88	0.081	629.5	61	3.4	72.64	98.5
P2	7.43	25.90	28.20	988	6.94	114	55.5	6.42	0.039	416.2	59.2	7.33	132.62	31.2
P3	7.41	29.90	32.50	847	6.1	127	28.4	5.84	0.025	284.12	41.3	3	84.62	32.84
P4	7.61	22.50	36.00	622	7.33	28.68	54.85	3	0.018	342.82	74	3.5	52.10	32.8
P5	7.52	25.90	30.00	594	8.36	25.63	51.02	7.45	0.028	296.3	52.63	1.53	65.33	25.2
P6	7.82	26.20	29.80	542	8.41	14.62	53.94	8.2	0.045	250.4	24.2	1.69	65.8	21.38
P7	7.22	26.40	32.00	935	7.44	92.48	45.5	8.5	0.023	352	89.62	1.3	64.13	33.72
P8	7.76	29.90	32.00	894	7.15	66.8	41.3	8.5	0.042	300.24	32	1.1	72.14	39.2
P9	7.14	25.10	29.50	1186	8.32	26.42	76.15	14	0.033	369.6	46	3.1	80.16	39.2
P10	7.59	28.50	30.50	816	7.93	76.14	28.4	6.8	0.056	284.26	20	2.7	68.14	40.4
P11	7.63	26.50	30.00	965	6.08	57	101.175	6.45	0.083	334.28	95.4	2.8	58.6	23.1
P12	7.51	27.60	28.70	1128	6.92	162.4	81.65	26.16	1.056	463.6	72.8	2.9	117.6	39.6
P13	7.59	30.50	31.50	844	6.04	110.6	59.2	17.4	0.057	312.1	74	3.6	68.4	20.95
P14	7.98	25.20	27.00	1223	7.39	172.6	123.4	4.5	0.045	345.9	59	3.4	98.4	49.3
P15	7.68	25.40	29.20	3750	8.1	473.2	982.1	14.5	0.028	443.5	412.5	21	252.6	141.5
P16	7.36	22.70	20.70	6400	6.42	327.3	1822.5	30.7	0.052	462.8	845	25	362.5	210.8
P17	7.60	29.30	30.50	635	7.26	27.8	62.6	2.84	0.072	292.8	67	2.3	58.12	24.8
P18	7.41	29.90	32.50	847	6.1	42.5	83.9	13.14	0.069	391.62	64.2	1.2	81.5	45.3
P19	7.59	28.50	29.50	816	7.93	31.92	76.8	5.4	0.037	385.52	42.8	2.8	79.6	50.1

Water chemistry study

Piper method

The studied groundwater chemical nature, during rainy and drought periods, is illustrated in the Piper diagrams (Fig. 6).

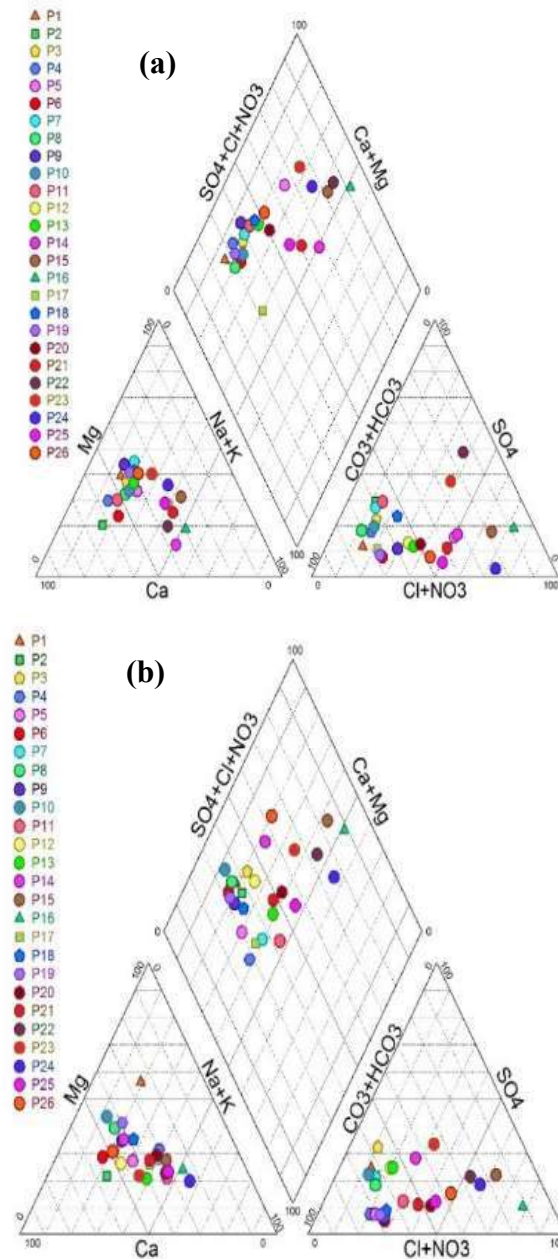


**Figure 6.** Piper diagrams for all S-M region water categories at (a) winter (January 2018), and (b) summer (July 2018).

This representation focused on 26 samples taken at the different sampling points, during the S-M region waters physicochemical quality monitoring. It was observed that  $\text{CO}_3^{2-}$  and  $\text{HCO}_3^-$  are the dominant anions, for approximately 80% of the analyzed water samples, while the remaining 20% are the dominant  $\text{SO}_4^{2-}$  and  $\text{Cl}^-$  anions. In addition, 75% of the analyzed water have no dominant cation, although the remaining 25% have dominant  $\text{Na}^+$ . It is noted that the facies of these water

samples are Ca and magnesium bicarbonate ( $Mg(HCO_3)_2$ ), probably due to the schist formations in south S-M [16], with a slight tendency towards the Ca facies. Thus, the Cl and  $SO_4^{2-}$  facies of the studied waters are probably due to the gypsum lens dissolution located in the Miocene marl formations and/or to the leaching of agricultural lands following the water infiltration into the aquifer. It is known that the groundwater quality is influenced by many factors, such as chemistry, the reservoir rocks geology [17] and anthropogenic factors [18].

Schoeller-Berkaloff method

The water physicochemical analysis results obtained, in the S-MD region, at winter and summer, presented in Tables 1 and 2, are graphically represented by the Schoeller-Berkaloff (S-B) logarithmic diagram (Figs. 7 and 8).

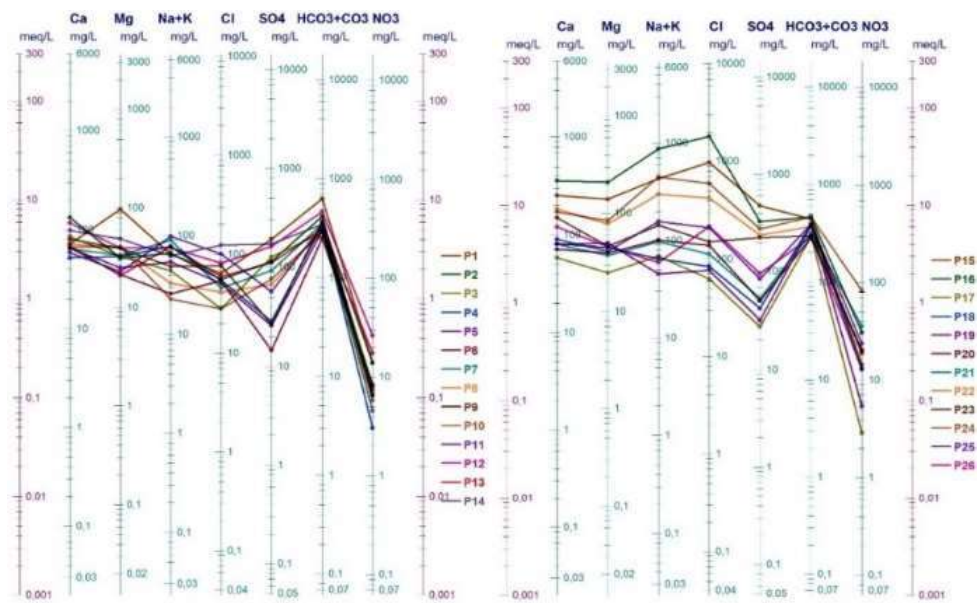


Figure 7. S-M region groundwater S-B diagram, at winter (January 2018).

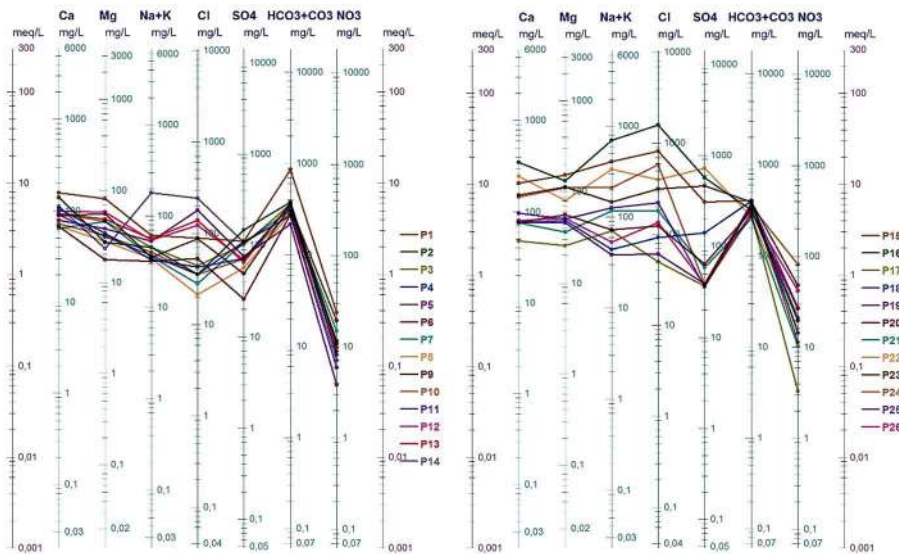


Figure 8. S-M region groundwater S-B diagram, at summer (July 2018).



The obtained results confirm the chemical facies already highlighted by the Piper graphic representation of, namely, Ca and Mg(HCO<sub>3</sub>)<sub>2</sub>, with a slight tendency towards the Cl facies.

### Sodium adsorption ratio

SAR is an important parameter to determine the irrigation groundwater suitability, because it measures the danger that alkali Na can represent to the crops. So, Na enters the aquifer through rain and rock dissolution. Due to its effects on soils and plants, it is considered among the main factors governing irrigation water. This ratio is determined as follows:

$$SAR = \frac{Na^+}{\sqrt{\frac{(Ca^{2+} + Mg^{2+})}{2}}} \quad (1)$$

The obtained results of the S-M region groundwater are indicated in Table 3.

**Table 3.** Statistical summary of Na%, Mg%, SAR and RSC irrigation water quality indices.

Wells	SAR	Mg%	Na%	RSC
P1	0.90808663	46.5134316	15.3123778	-0.47226667
P2	0.90613085	24.6252216	17.778108	-3.1497623
P3	0.92640666	45.7317671	19.0719295	-2.53369454
P4	0.67820366	35.0627667	15.1497083	-2.3255
P5	1.22847576	44.7192904	25.0925902	-3.58183333
P6	0.8759078	30.4474892	22.4853992	-0.28741667
P7	0.79665611	54.7782918	18.15212	-2.0504
P8	0.85883046	40.614977	20.9136721	-1.0968
P9	0.68304203	51.3894351	14.5517188	-3.48930546
P10	0.94568275	42.9739785	21.8090305	-1.46553333
P11	0.84154669	36.9024857	18.6477915	-2.75979781
P12	1.06425847	49.2143943	19.8530226	-3.94860656
P13	1.17784416	46.9554739	22.4684468	-2.61995956
P14	4.09051108	25.6769621	51.6658804	-3.13697049
P15	5.35417842	55.3292046	44.3254675	-16.3831667
P16	8.3027562	38.9087902	52.51428	-23.3184749
P17	2.05136534	47.0382252	40.9850754	0.09936667
P18	0.94102248	51.4600897	19.857536	-1.24426667
P19	0.83975364	49.8621767	18.3247984	-1.37426667
P20	1.54635851	55.0333034	27.7472664	-3.32005902
P21	2.87010919	44.4444444	44.1120018	-2.55
P22	4.93730561	35.32004	44.6115989	-14.5843224
P23	2.21559303	55.2154896	27.7939419	-10.7001907
P24	3.31494019	56.281407	36.6777363	-10.8433333
P25	2.69344553	46.8137183	38.9102689	-3.20293333
P26	1.11695079	51.5971258	22.1627834	-3.3952541

The waters of the different studied sites showed that SAR varied from 0.8 meq/L (milliequivalents per liter) (P9) to 5.35 meq/L (P16), and from 0.84 meq/L (P6) to 6.5 meq/L (P16), during summer and winter, respectively.

On the other hand, taking into account the SAR evolution vs. EC presented in Fig. 9, it can be deduced that, in July 2018, the water samples belonged to the following salinity (C) and sodicity (S) classes: 69% to C3S1 (average to poor); 17% to C2S1

(good to average); and 14% to C4S1 (poor to bad), C4S2 (very bad) and C4S4 (not recommended for irrigation).

However, in January 2018, the water samples belonged to the following classes: 15% to C2S1 (good to average); 71% to C3S1 (average to poor); and 14% to C4S1 and C4S2 (poor to very bad).

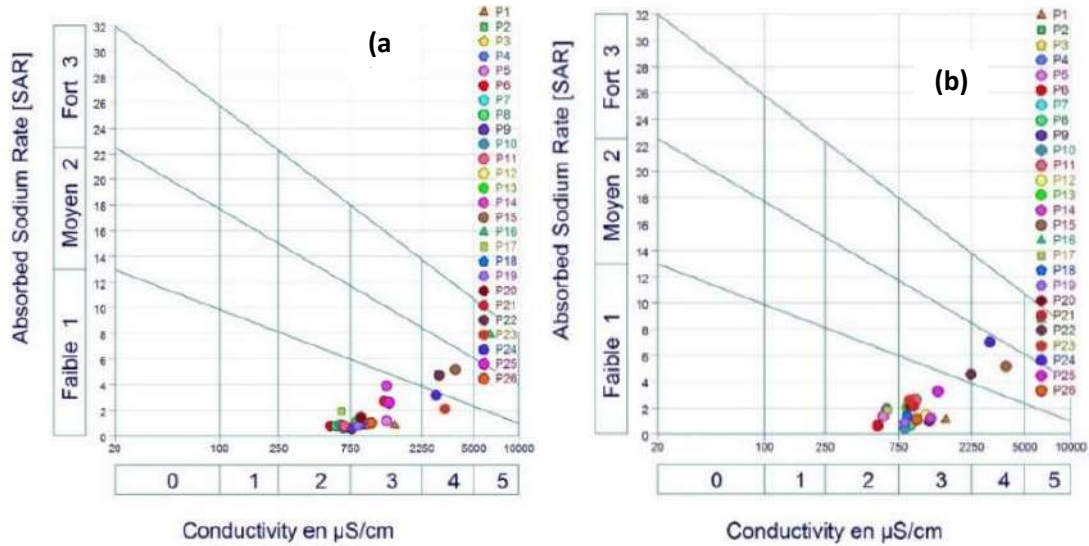


**Figure 9.** S-M region groundwater riverside diagrams at (a) winter (January 2018) and (b) summer (July 2018).

Additionally, C and S water classes interpretation obtained throughout the study period is summarized in Table 4.

**Table 4.** Tested groundwater salinity (C) and sodicity (S) classes interpretation, at winter and summer, according to Wilcox’s diagram.

Classes of salinity (C) and sodicity (S)	Using state
C2S1	Good to medium quality water to be used with caution for poorly drained soils and sensitive plants.
C3S1	Medium to poor quality water to be used with caution; requires drainage with leaching and/or gypsum additions.
C3S2 and C4S1	Poor to very poor quality water, to be used with care for heavy soils and sensitive plants; the use for light and well-drained soils requires leaching and/or gypsum supply.
C4S2	Very poor quality water to be only used for light and well-drained soils and for resistant plants which need leaching and/or gypsum additions.
C3S4	Very bad quality water to be only used for exceptional circumstances.
C4S4	Water not recommended for irrigation.

Na percentage

Na<sup>+</sup> ion is an important cation in the agriculture field, which deteriorates the soil structure and reduces the crop yield. In fact, when its concentration is high in the irrigation water, it tends to be absorbed by the clay particles and replaced by Mg<sup>2+</sup> and Ca<sup>2+</sup> ions. This exchange process in the soil reduces its permeability.

Therefore, Na% is considered an important index for irrigation water assessment. It is determined according to the formula:

$$Na\% = \frac{(Na^+ + K^+)}{Ca^{2+} + Mg^{2+} + Na^+ + K^+} \times 100 \quad (2)$$

The results recorded in Table 5 summarize the information about the irrigation groundwater quality from the Na% evolution, according to Wilcox (1948). It is shown, for winter and summer, that Na% values range from 20 to 42%. According to Table 5, a Na% < 40% value indicates that the water is suitable for irrigation.

**Table 5.** Irrigation groundwater quality from the Na% evolution.

Seasons	Classes	Na%	Water Quality	Wells%
Winter	C1	Na ≤ %20	Excellent quality agriculture water	15%
	C2	20 < Na% ≤ 40	Good quality agriculture water	62%
	C3	40 < Na% ≤ 60	Acceptable quality agriculture water	23%
Summer	C1	Na% ≤ 20	Excellent quality agriculture water	42%
	C2	20 < Na% ≤ 40	Good quality agriculture water	38%
	C3	40 < Na% ≤ 60	Acceptable quality agriculture water	20%
	C4	60 < Na% ≤ 80	Poor quality agriculture water	0%
	C5	Na% > 80	Bad quality agriculture water	0%

In addition, the results projection on the Riverside (1954) and Wilcox’s diagrams (Fig. 10) showed that the majority of wells are of good quality, except P15, P16 and P23, which are of poor quality, because they are very mineralized. These observations were confirmed by other authors, which have shown that poor quality water is salty/loaded and has high EC [19]. In addition, other work realized in Algeria revealed that there is a high risk of soil salinization by the use of water with high mineralization.

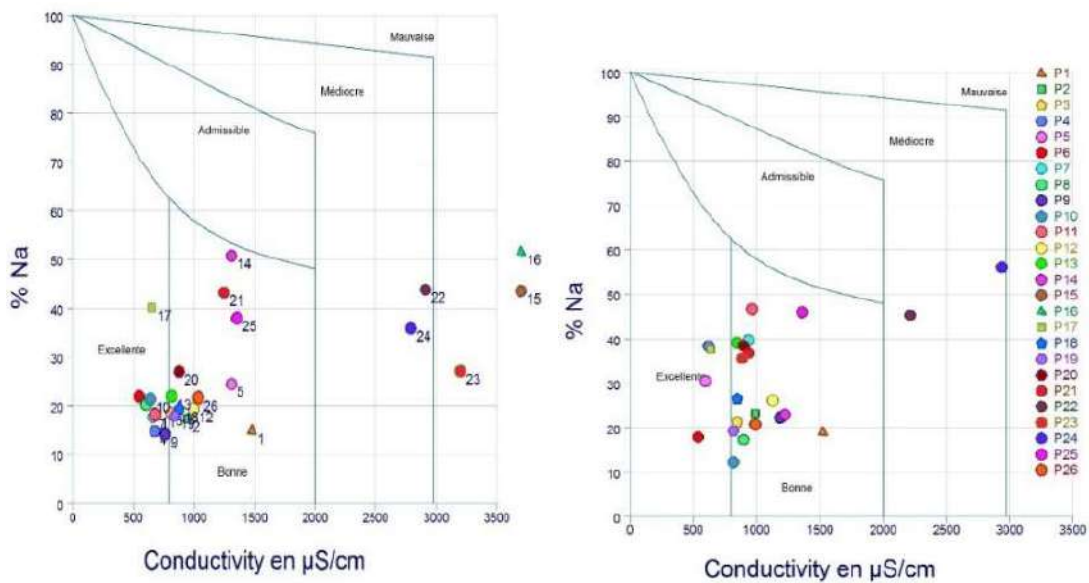


**Figure 10.** Wilcox’s diagram showing the irrigation groundwater suitability at (a) winter (January 2018) and (b) summer (July 2018) [20].

Mg percentage

The calculated Mg% values from the groundwater of the studied area are presented in Table 3. It was found that the obtained values ranged from 24 to 56%. So, eight wells (30.7%) have Mg% values superior to 50%, which makes the groundwater unsuitable for irrigation, while eighteen samples (60.3%) are suitable for irrigation, as indicated in Table 6 [21].

Table 6. Irrigation groundwater quality, according to Mg% values.

Permissible range	Class	Wells%
Mg% < 50	Suitable for irrigation	60.3
Mg% > 50	Unsuitable for irrigation	30.7

Residual sodium carbonate (RSC)

RSC is another significant parameter to determine if the water is suitable for irrigation. It determines the HCO<sub>3</sub><sup>-</sup> and CO<sub>3</sub><sup>2-</sup> ions dangerous effects on the water quality. So, this RSC index was estimated by using the equation [22]:

$$RSC = (CO_3^{2-} + HCO_3^-) - (Ca^{2+} + Mg^{2+}) \quad (3)$$

where all ionic concentrations are expressed in meq/L.

Based on the RSC, Lloyd and Heathcote (1985) have classified irrigation water as: good, when it is inferior to 1.25 meq/L; poor, when it ranges from 1.25 to 2.5 meq/L; and not recommendable, when it is superior to >2.5 meq/L. According to the obtained RSC values in our study, all groundwater samples are suitable for irrigation.

*Principal component analysis (PCA)*

The principal component analysis is a multivariate statistical tool used to analyze the variability of a dataset. Several studies have used PCA in surface and groundwater studies [23-25].

For this study, the principal component analysis was carried out for 26 samples and 12 variables (pH, T°, EC, NO<sub>3</sub><sup>-</sup>, NO<sub>2</sub><sup>-</sup>, Cl<sup>-</sup>, HCO<sub>3</sub><sup>-</sup>, SO<sub>4</sub><sup>2-</sup>, Ca<sup>2+</sup>, Mg<sup>2+</sup>, K<sup>+</sup> and Na<sup>+</sup>). Fig. 11 represents the principal factors corresponding to the different variation sources in the data set.

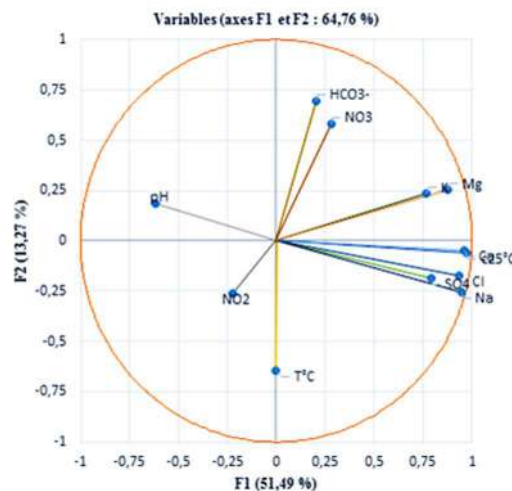


Figure 11. Correlation plot among variables and factor loading.

Table 7 summarizes PCA results and the variance induced by each of the principal components. The PCA rendered three principal components that contributed to the total variance of over 74.93%, such as F1 (51.49%), F2 (13.26%) and F3 (10.18%).

**Table 7.** Values and percentages expressed for the main axes.

	F1	F2	F3
Proper value	6.179	1.592	1.222
Variability(%)	51.490	13.266	10.181
Cumulative(%)	51.490	64.755	74.937

On the other hand, Table 8 shows that the F1 axis is strongly positively correlated with T (C)<sup>o</sup>, NO<sub>3</sub><sup>-</sup>, Cl<sup>-</sup>, Na<sup>+</sup>, HCO<sub>3</sub><sup>-</sup>, SO<sub>4</sub><sup>2-</sup>, Ca<sup>2+</sup>, Mg<sup>2+</sup> and K<sup>+</sup>. This axis expresses both water mineralization and organic pollution, which aggregates the major cations. In addition, the gathering of these last elements around the F1 axis showed that they would be identical phenomena, but occurring by different mechanisms. So, the Ca<sup>2+</sup>, Mg<sup>2+</sup>, K<sup>+</sup>, Cl<sup>-</sup>, Na<sup>+</sup> and HCO<sub>3</sub><sup>-</sup> ions could result from the rocks hydrolysis and minerals decomposition, in the S-M region, through redox reactions, ion exchange, precipitation and/or adsorption. The presence of SO<sub>4</sub><sup>2-</sup>, NO<sub>3</sub><sup>-</sup> and NO<sub>2</sub><sup>-</sup> ions could have a mainly anthropogenic origin, either by leaching of fertilizers spread, domestic wastewater discharges, and/or by organic matter degradation. This would mean pluvio-lessivage of the grounds [26]. So, F1 axis is correlated with natural origin mineralization (water-rock contact or residence time) and anthropogenic (soils pluvio-lessivage) factors. Conversely, the F2 axis is quite negatively correlated with T (C)<sup>o</sup>, Cl<sup>-</sup>, SO<sub>4</sub><sup>2-</sup> and Na. In addition, it is positively correlated with nitrate NO<sub>3</sub><sup>-</sup>, ammonium, HCO<sub>3</sub><sup>-</sup>, Ca and hardness (mainly related to the Ca and Mg amount in the water). This axis expresses less water mineralization than that of other axes [26].

**Table 8.** Correlation analysis of the physiochemical parameters for groundwater samples.

Variables	pH	T °C	CE (25 °C)	SO42-	Cl-	NO3-	NO2-	HCO3-	Na+	K+	Ca2+	Mg2+
Ph	1											
T °C	-0.172	1										
CE (25 °C)	-0.535	-0.038	1									
SO42-	-0.369	-0.011	0.774	1								
Cl-	-0.580	0.075	0.962	0.640	1							
NO3-	-0.016	-0.281	0.324	0.068	0.249	1						
NO2-	0.161	0.009	-0.093	-0.106	0.148	-0.123	1					
HCO3-	-0.169	-0.147	0.071	-0.005	0.022	0.181	-0.155	1				
Na+	-0.571	0.114	0.953	0.752	0.969	0.154	-0.125	-0.050	1			
K+	-0.397	-0.088	0.677	0.521	0.646	0.021	-0.243	0.514	0.656	1		
Ca2+	-0.574	-0.007	0.925	0.844	0.875	0.184	-0.267	0.187	0.914	0.714	1	
Mg2+	-0.439	-0.086	0.863	0.620	0.791	0.501	-0.147	0.315	0.756	0.675	0.767	1

## Conclusion

The problems encountered in the S-M region include drought, wastewater evacuation and the industrial and high demand for agricultural water. The irrigation groundwater quality in this region, during 2018, was investigated using hydrogeochemical and statistical methods. It was found that 14% of the analyzed wells are not suitable for irrigation, while the rest are generally of good quality and

suitable for it. In addition, it was found that 30% of wells have a Mg risk, and 20% have a high Na adsorption rate. Therefore, if the water is not properly treated before its use for irrigation, it can make the soil more alkaline and, eventually, lead to clogged pores and low crop yield.

However, the hydrogeochemical analysis revealed that a hydrogeochemical-dominated groundwater facies is composed by genetic types of Ca-Mg-HCO<sub>3</sub> and Ca-Mg-Cl-SO<sub>4</sub> water. Additionally, the groundwater chemistry is largely controlled by ion-exchange reactions facilitated by the minerals weathering in the studied region. A certain level of anthropogenic pollution contribution, in particular, agricultural pollution, was confirmed by the multivariate statistical study.

### Authors' contributions

**M. Doubi:** conceived and designed the analysis; collected the data; wrote the paper. **H. Darif:** collected the data; inserted data or analysis tools; performed the analysis. **A. Koulou:** conceived and designed the analysis; collected the data; wrote the paper. **R. Touir:** conceived and designed the analysis; collected the data; inserted data or analysis tools; performed the analysis; wrote the paper. **H. Abba:** conceived and designed the analysis; collected the data; inserted data or analysis tools. **M. Khaffou:** collected the data; inserted data or analysis tools. **H. Erramli:** conceived and designed the analysis; collected the data; inserted data or analysis tools; performed the analysis.

### References

1. Selvakumar S, Chandrasekar N, Kumar G. Hydrogeochemical characteristics and groundwater contamination in the rapid urban development areas of Coimbatore, India. *Water Resour Ind.* 2017;17:26-33. <https://doi.org/10.1016/j.wri.2017.02.002>
2. Njimat S, Griou H, Doubi M, et al. Fertilizing power study of wastewater From Dar El Gueddari WWTP-Grain Corn Case. *Indian J Environmen protect.* 2019;39(9):839-843. <http://dx.doi.org/10.13005/ojc/370213>
3. Pulido-Bosch A, Rigol-Sanchez JP, Vallejos A, et al. Impacts of agricultural irrigation on groundwater salinity. *Environ Earth Sci.* 2018;77:197. <https://doi.org/10.1007/s12665-018-7386-6>
4. Faunt CC, Sneed M, Traum J, et al. Water availability and land subsidence in the Central Valley, California, USA. *Hydrogeol J.* 2016;24:675-684. <https://doi.org/10.1007/s10040-015-1339-x>
5. Konikow LF, Kendy E. Groundwater depletion: A global problem. *Hydrogeol J.* 2015;13:317-320. <https://doi.org/10.1007/s10040-004-0411-8>
6. Rodell M, Velicogna I, Famiglietti JS. Satellite-based estimates of groundwater depletion in India. *Nature.* 2009;460:999-1002. <https://doi.org/10.1038/nature08238>
7. Islam A, Rakib MA, Islam M, et al. Assessment of health hazard of metal concentration in groundwater of Bangladesh. *Am Chem Sci J.* 2015;5(1):41-49.
8. Bodrud-Doza Md, Towfiqul Islam A, Ahmed F, et al. Characterization of groundwater quality using water evaluation indices, multivariate statistics and geostatistics in central Bangladesh. *Water Sci.* 2016;30:19-40. <https://doi.org/10.1016/j.wsj.2016.05.001>

9. Bhuiyan M, Dampare S, Islam M, et al. Source apportionment and pollution evaluation of heavy metals in water and sediments of Buriganga River, Bangladesh, using multivariate analysis and pollution evaluation indices. *Environ Monit Assess.* 2015;187:4075. <https://doi.org/10.1007/s10661-014-4075-0>
10. Rahman M, Saadat A, Islam M, et al. Groundwater characterization and selection of suitable water type for irrigation in the western region of Bangladesh. *Appl Water Sci.* 2014. <http://dx.doi.org/10.1007/s13201-014-0239-x>
11. Bouchaou L, Michelot J, Vengosh, et al. Application of multiple isotopic and geochemical tracers for investigation of recharge, salinization, and residence time of water in the Souss-Massa aquifer, southwest of Morocco. *J Hydrol.* 2008;352:267-287. <https://doi.org/10.1016/j.jhydrol.2008.01.022>
12. Bouragba L, Mudry N, Bouchaou L, et al. Characterization of groundwater in the Souss upstream basin: Hydrochemical and environmental isotopes approaches. *Afr J Env Sci Tech.* 2011;5(4):307-315.
13. Hssaisoune M, Boutaleb S, Benssaou M, et al. Geophysical and structural analysis of the Souss-Massa aquifer: synthesis and hydrogeological implications. *Geo-Eco-Trop.* 2012;36:63-82.
14. Doubi M, Dermaj A, Ait Hadou B, et al. Contribution to the Study of Physical and Chemical Oued Moulouya and those Influential in the region Outat of el Haj. *Larhyss J.* 2013;16:91-104.
15. Holland, HD. *The Chemistry of the Atmosphere and Oceans.* John Wiley and Sons, New York, 1978; pp. 351.
16. Drouiche A, Zahi F, Debieche T, et al. Hydrogeological and hydrochemical characterization of the waters of the swampy area of el-kennar (Jijel, N-E Algerien). *Algerie Equipement.* 2019;60:29-40.
17. Emenike C, Tenebe I, Ngene B, et al. Accessing safe drinking water in sub-Saharan Africa: issues and challenges in south-west Nigeria. *Sustain Cities Soc.* 2017;30:263-272. <https://doi.org/10.1016/j.scs.2017.01.005>
18. Frape S, Fritz P, McNutt R. Water-rock interaction and chemistry of groundwater from the Canadian shield. *Geochem Cosmochim Acta.* 1984;48:1617-1627. [https://doi.org/10.1016/0016-7037\(84\)90331-4](https://doi.org/10.1016/0016-7037(84)90331-4)
19. Rouabhia A, Djabri L. L'irrigation et le risque de pollution saline. Exemple des eaux souterraines de l'aquifère miocène de la plaine d'El Ma Labiod. *Larhyss J.* 2010;8:55-67.
20. Wilcox L. *Classification and use of irrigation waters.* Washington: US Department of Agriculture, 1995; pp. 19.
21. Szabolcs I, Darab C. The Influence of Irrigation Water of High Sodium Carbonate Content of Soils. *Proceedings of 8th International Congress of ISSS, Trans II, 1964; 803-812.* <http://real.mtak.hu/id/eprint/96046>
22. Eaton F. Significance of Carbonates in Irrigation Waters. *Soil Sci.* 1950;69:123-134. <https://doi.org/10.1097/00010694-195002000-00004>
23. Abou Zakhem B, Al-Charideh A, Kattaa B. Using principal component analysis in the investigation of groundwater hydrochemistry of Upper Jezireh Basin. *Syria Hydrol Sci J.* 2017;62:2266-2279. <https://doi.org/10.1080/02626667.2017.1364845>

24. Guan H, Hutson J, Ding Z, et al. Principal component analysis of watershed hydrochemical response to forest clearance and its usefulness for chloride mass balance applications. *Water Resour Res.* 2013;49:4362-4378. <https://doi.org/10.1002/wrcr.20357>
25. Ravikumar P, Somashekar R. Principal component analysis and hydrochemical facies characterization to evaluate groundwater quality in Varahi river basin, Karnataka state, India. *Appl Water Sci.* 2017;7:745-755. <https://doi.org/10.1007/s13201-015-287-x>
26. Lemacha H, Taouil H, Doubi M, et al. A study on ground water geochemistry and metallic properties in the Guir Basin (Eastern Morocco). *Int J Adv Res.* 2017;5(10):1023-1029.